

Constraining variations of dust properties in circumstellar disks with mm observations



F. Trotta(Arcetri/ESO), T.Birnstiel(MPIA), L.Ricci(ESO), C.P.Dullemond(MPIA), A.Natta(Arcetri), L.Testi(ESO/Arcetri)



Abstract

We present initial results of including radial dependent grain growth at the midplane of two layers passive disks. Our models predict variations of the disk emission as a function of radius as a consequence of the different grain distribution as a function of radius. These variations are within the limits set by current spatially resolved multi wavelength observations of protoplanetary disks, but will be readily observable with the next generation of (sub)millimeter telescopes, EVLA and ALMA

Introduction

Grain growth in protoplanetary disks is the first step towards the formation of the rocky cores of planets. Models predict that grains grow, migrate and fragment in the disk and predict varying dust properties as a function of radius, disk age and physical properties.

To constrain grain growth and migration in protoplanetary disks high-angular resolution observations at more than one (sub-)mm wavelength are currently being performed to detect possible radial variations of the dust properties.

We have modified simple two-layer disk models (Chiang & Goldreich 1997, Dullemond, Dominik and Natta 2001) to include surface density profiles with exponential outer edges (as opposite to a sharp cutoff) and to allow for radial variation of the dust properties. The aim is to compare the prediction of these models against spatially resolved multi-frequency observations of disks.

Disk Model

We adopt the two-layer approximation of Chiang & Goldreich (1997) with the modifications of Dullemond, Dominik & Natta (2001). These models solve the radiation transfer in a simple way, and allow a self-consistent computation of the geometry of the disk. The main advantage of these models is the fast computation times, which allow for an efficient fitting of visibility datasets even allowing for the computation of large grids of model parameters. In spite of the simple radiative transfer approach, these models retain a high accuracy in predicting the millimeter emission from the disk midplane

We use a similarity solution for the disk surface density of a viscous Keplerian disk (Lynden-Bell & Pringle 1974) that has the characteristic of falling off exponentially at large disk radii. These models have been recently demonstrated to more accurately reproducing the observed dust distribution in protoplanetary disks (Hughes et al. 2008; Isella et al. 2009; Andrews et al. 2009)

For the dust model we consider spherical porous grains made of 7% of silicates, 21% amorphous carbonaceous, 42% water ice and 30% vacuum (simplification of the dust model considered in Pollack et al. 1994).

For the grain size distribution we use (part of) the dust evolution model of Birnstiel et al. (2010). This model solves the coagulation equation with 3 different sources for relative velocity of the particles: the Brownian motion, differential settling and turbulent mixing. Moreover it considers the fragmentation process.

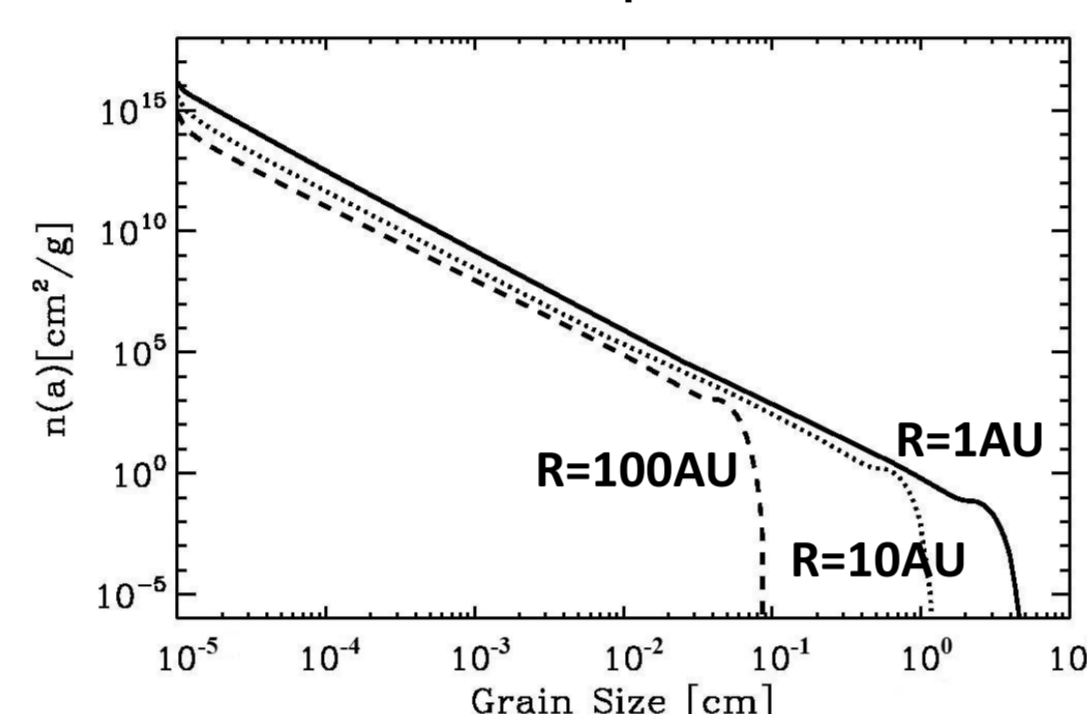
In order to use the model predictions and interpret the observations we have included in our disk model the possibility to have a radial variation of the dust properties. In particular, the possibility to modify the grain size distribution depending on the location in the disk

Fiducial Model

As fiducial parameters for our models we have used the following set:

Stellar Parameters		Disk Parameters	
Mass [M_{sun}]	0.5	Surface Density [g/cm^2] (Self-Similarity solution)	$\Sigma_{\text{gr}} = 23.8 \text{ gr}/\text{cm}^2$ $R_{\text{gr}} = 30 \text{ AU}$, $g = 1$ ($\rightarrow M_{\text{disk}} = 5 \times 10^{-2} M_{\text{sun}}$)
Radius [AU]	2	Dust to Gas ratio	10^{-2}
Effective Temperature [K]	4000	Dust density [g/cm^3]	1.2
		α -viscosity	10^{-3}
		Fragmentation velocity [cm/s]	3×10^2

We show in these plots the obtained dust properties in the disk

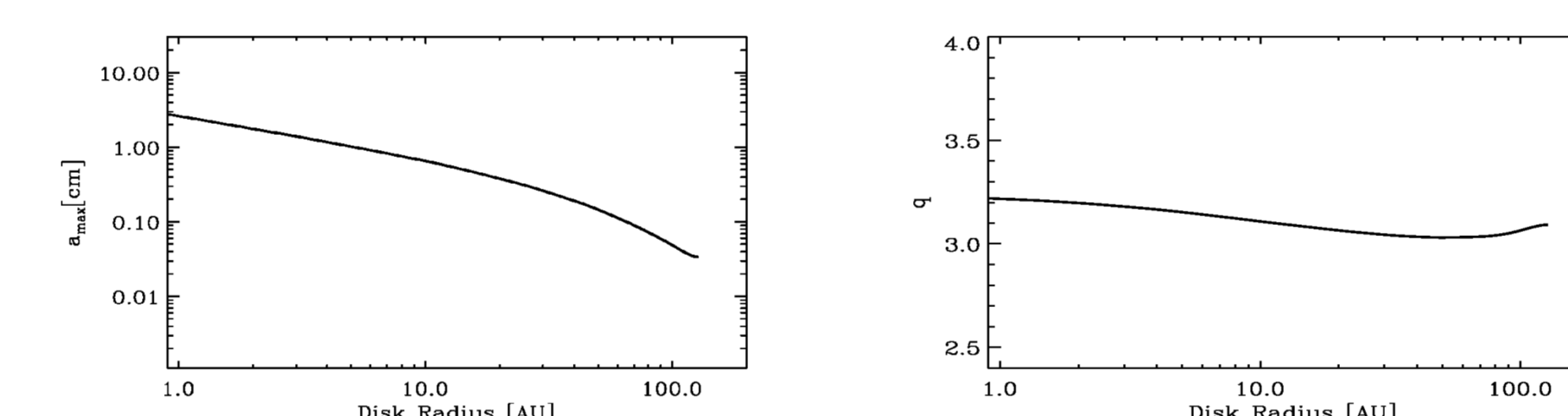


This plot shows the dust size distribution at three different radii: at a distance of 1 AU (solid line), 10AU (point line) and 100AU (dashed line) from the star

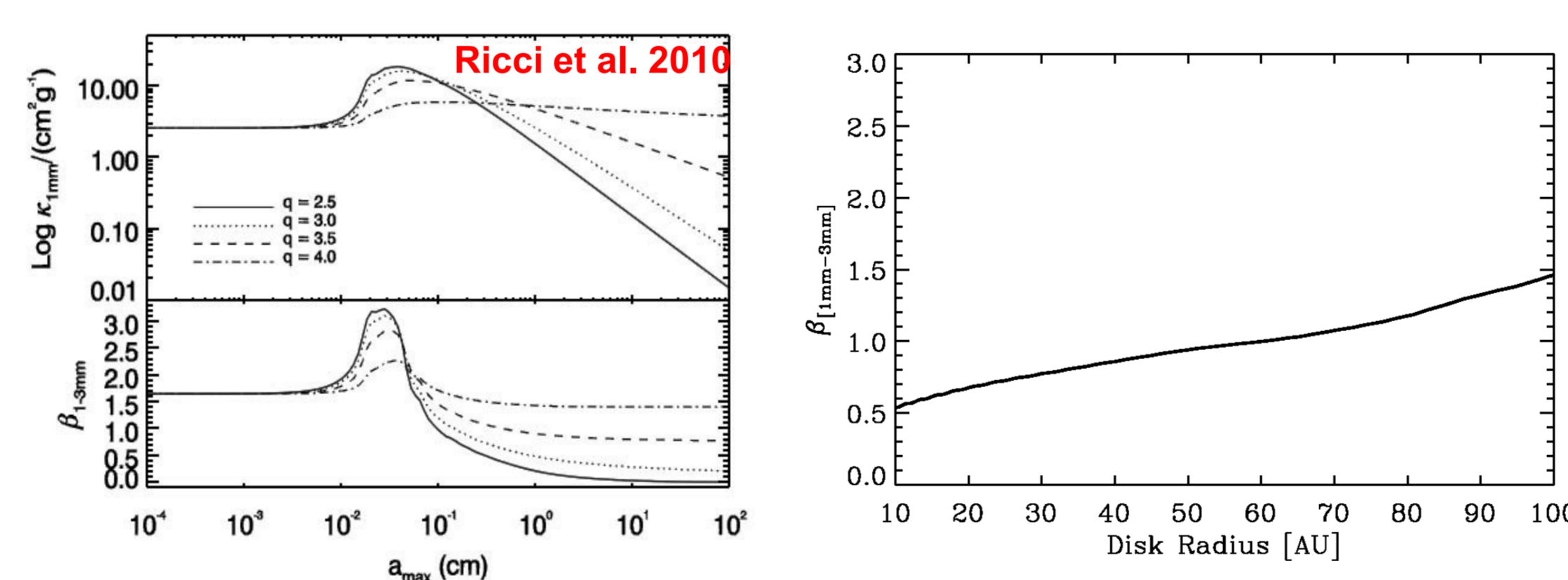
These distributions can be very well approximated by a truncated power law distribution approximation:

$$n(a) \propto a^{-q} \quad \text{with } 0.1 \mu\text{m} \leq a \leq a_{\text{max}}$$

The plots below show the radial profile of the maximum dust size (left) and the slope q (right) of power law function that we have obtained



In the plot below on the left we show the dust opacities and the slope (β) of the dust opacity between 1 and 3 mm for our dust model as a function of a_{max} and q (from Ricci et al. 2010). On the right we show the predicted value of β as function of radius in the disk as predicted by our fiducial model.



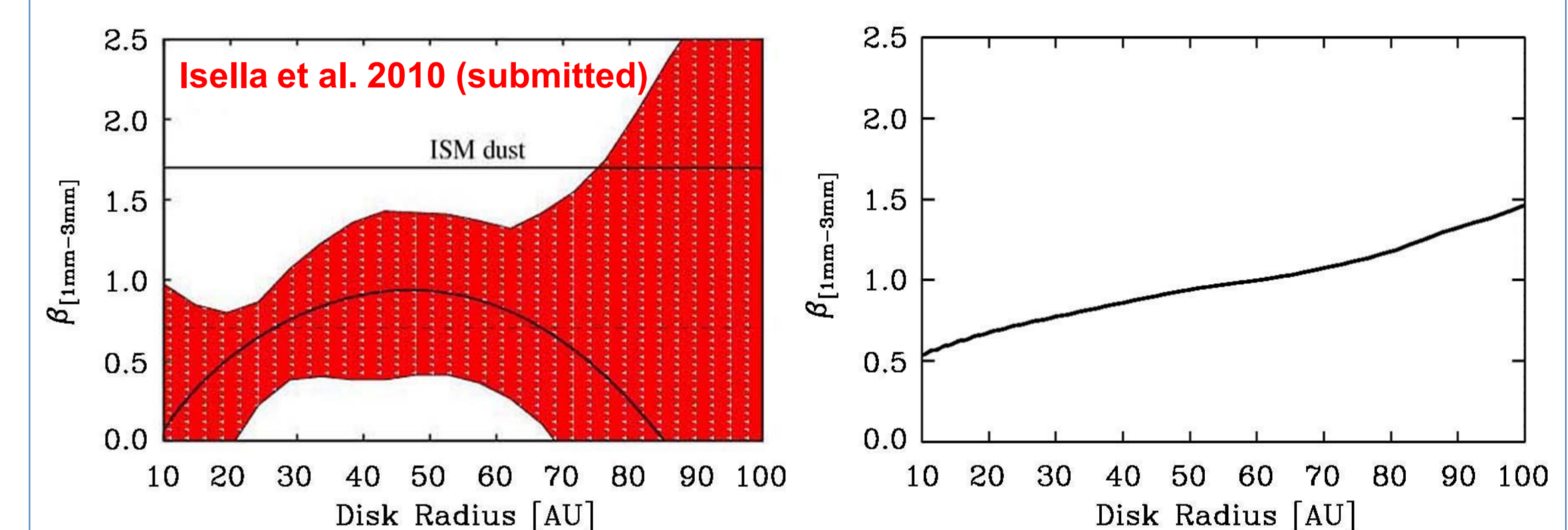
Constraining the dust properties with observations

One direct tool to investigate the grain growth in circumstellar disks around young stars is provided by resolved multi-wavelength images of the disk. At millimeter wavelengths, the dust thermal emission is generally optically thin and provides a measure of the radial distribution of the circumstellar dust. For such a study high angular resolution interferometry at mm-wavelengths is needed to spatially resolve the dust emission from the disk mid-plane.

Until now there have been only a few attempts to constrain the radial variation of dust properties with observations at mm-wavelengths. Very recently, Isella et al. (2010) have tried to put constraints on the dust properties variation within the protoplanetary disks around the young stars RY Tau and DG Tau with the CARMA Interferometer. Due to the large error bars they could only put limits on the possible variations (see Figure below for RY Tau)

To investigate the radial dependence of the dust opacity spectral index they firstly fit the CARMA maps at 1 and 3mm separately assuming a disk model (with a self-similar surface density) with constant dust properties throughout the disk. Then they compare the obtained two best-fit models at 1 and 3mm, and assuming that the discrepancies in the physical structure of the two models are due to a change in the dust opacity throughout the disk, they get constraints on $\beta(r)$.

Below we show the comparison between their results for RY Tau and our fiducial model



Black curved line: the best fit for the function $\beta(r)$ from the Isella analysis,
Red area: the area within 3σ from the best fit curve from his analysis,
Black straight line: ISM value of $\beta=1.7$

Function $\beta(r)$ we derived for our fiducial model

Future prospects

The investigation of the radial variation of β is still strongly limited by the relatively poor angular resolution and sensitivity of the current facilities. Observations with higher angular resolution and sensitivity are needed to place more stringent constraints on the radial variation of the dust opacity. For these purposes, the EVLA and ALMA arrays will play a crucial role in the next future.

In addition, much has to be done to really understand the grain growth process and the evolution of dust populations in disks. Our models assume that the expected fast radial drift of large grains is stopped, and thus they represent an ideal case for the presence of the largest possible particles in the disk at any given radius. How to stop the large grains from drifting towards the central star is as yet an unsolved problem. A tantalizing possibility is that grains are trapped in gas pressure maxima (e.g. spiral arms) within the disk. We are currently engaged in a program aimed at modeling this possibility and derive observational signatures that may be detectable with ALMA.

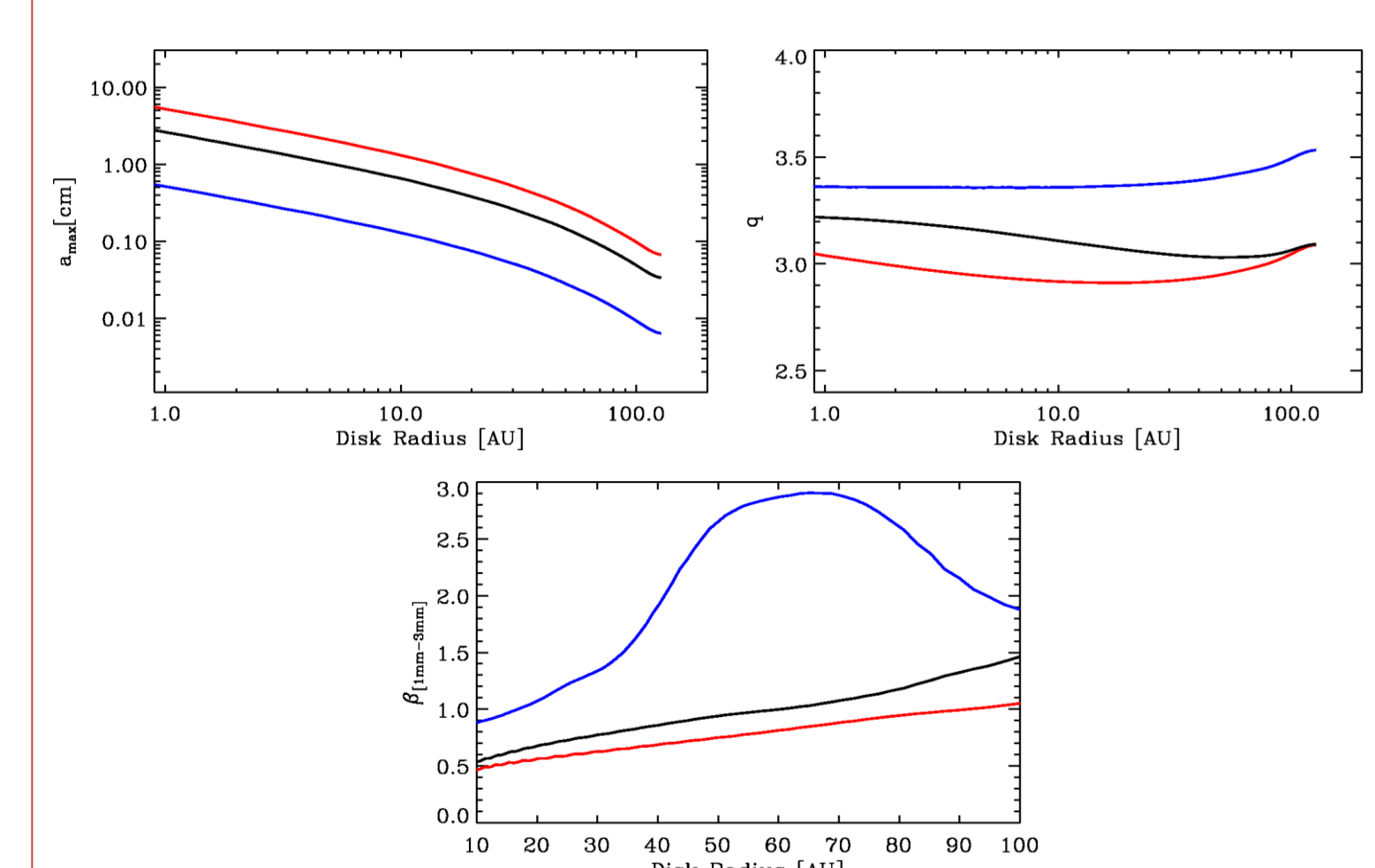
Comparison between different models

Now we show how the grain growth and the resulting β radial profile changes as compared to our fiducial model if we use different values for the main input parameters. The bump in β as a function of radius is produced because for some ranges of the parameters the value of a_{max} in some regions of the disk corresponds to the value for which the beta (a_{max}) function shown above has a peak ($0.1 \text{ mm} \leq a_{\text{max}} \leq 0.5 \text{ mm}$)

Effect of Turbulence

α -viscosity	5×10^{-4}	10^{-3}	5×10^{-3}
---------------------	--------------------	-----------	--------------------

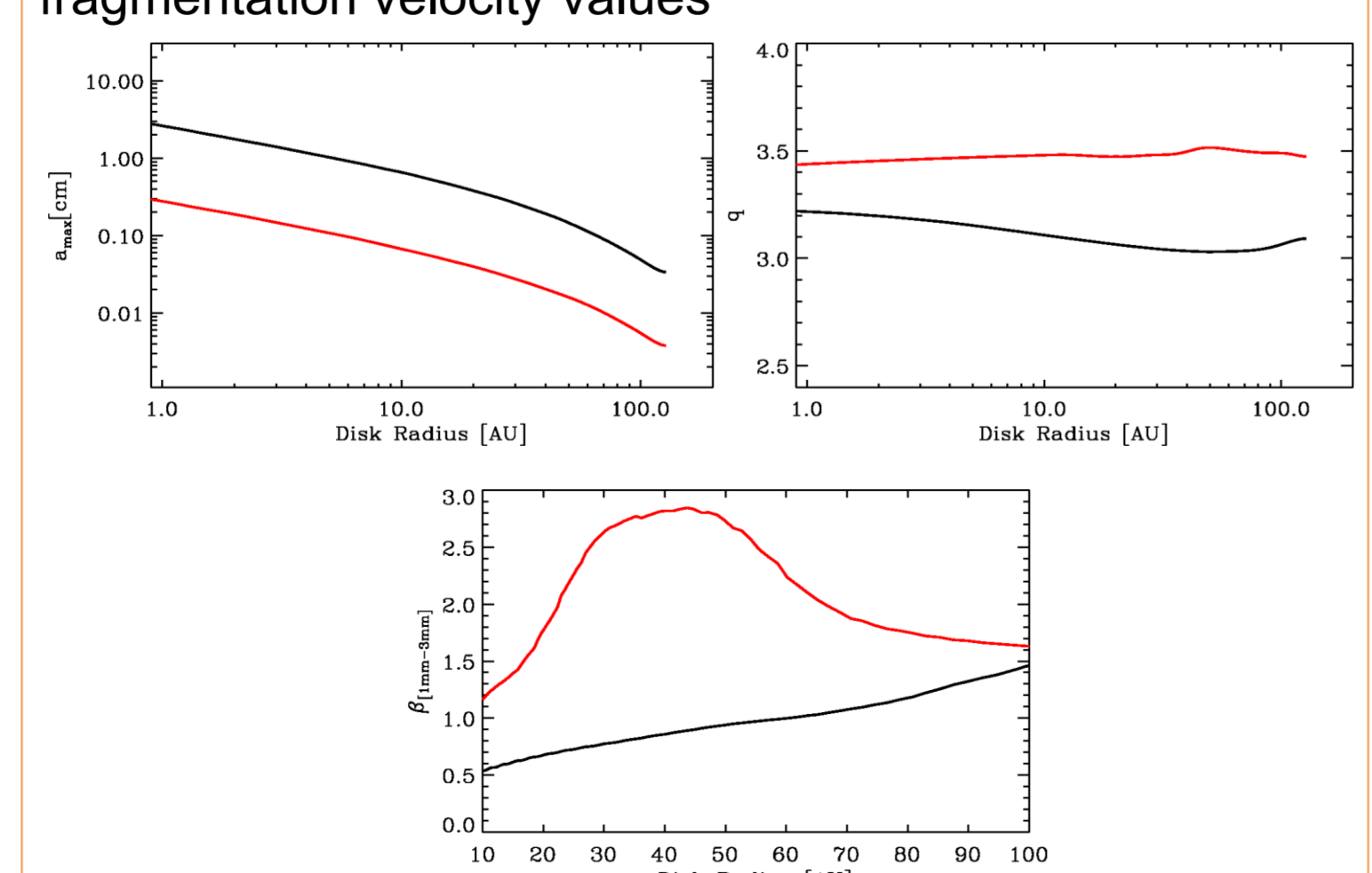
The plots below show the radial profile of the maximum dust size (top-left) and the slope q (top-right) of power law dust size distribution and the resulting dust opacity spectral index β (bottom) for the above α -viscosity values



Effect of Fragmentation Velocity

Fragmentation velocity [cm/s]	10^2	3×10^2
-------------------------------	--------	-----------------

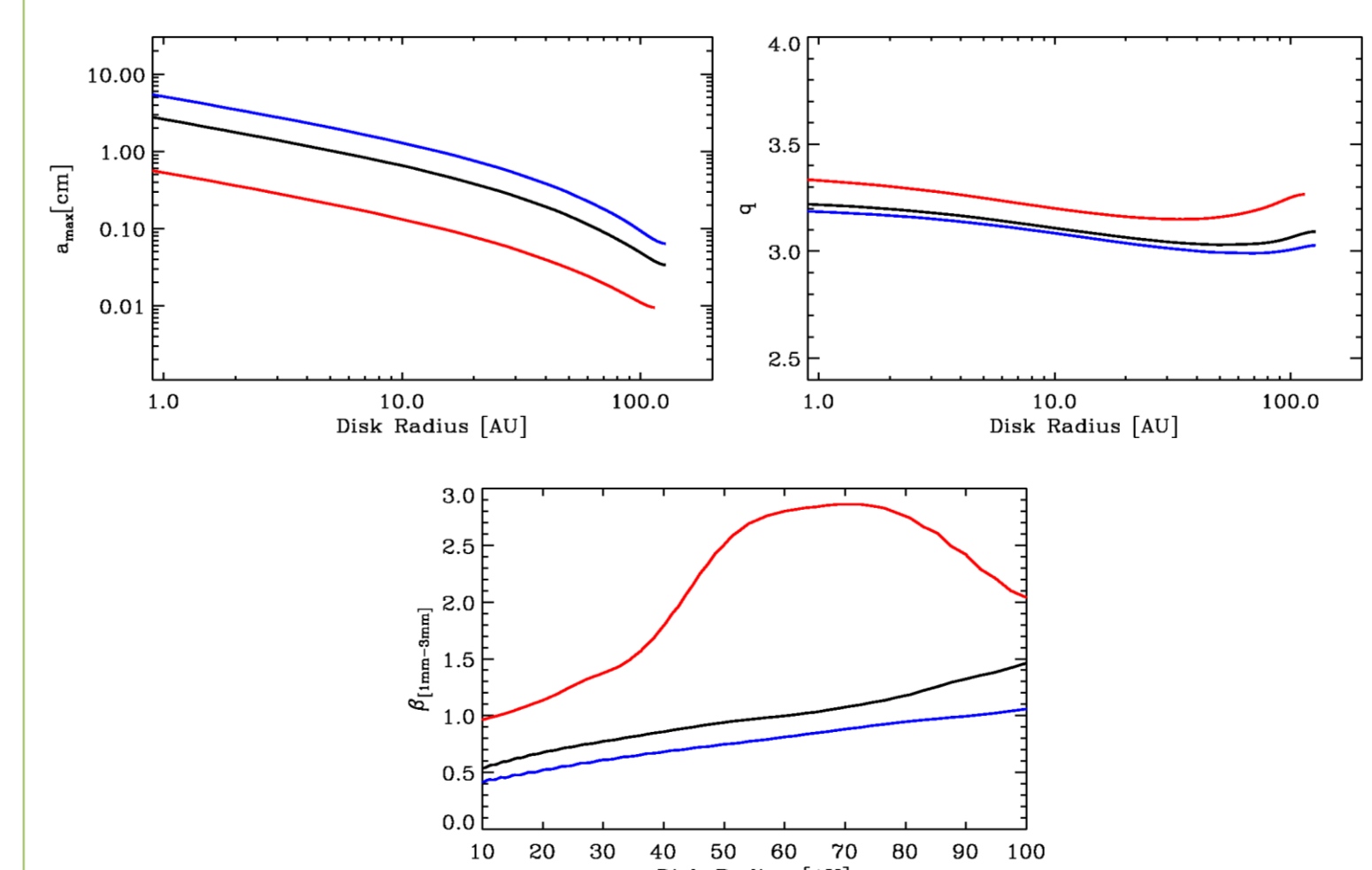
The plots below show the radial profile of the maximum dust size (top-left) and the slope q (top-right) of power law dust size distribution and the resulting dust opacity spectral index β (bottom) for the above critical fragmentation velocity values



Effect of Disk Mass

Disk Mass [M_{sun}]	10^{-2}	5×10^{-2}	10^{-1}
--------------------------------	-----------	--------------------	-----------

The plots below show the radial profile of the maximum dust size (top-left) and the slope q (top-right) of power law dust size distribution and the resulting dust opacity spectral index β (bottom) for the above disk mass values



A more detailed description of the models and results presented in this poster will appear in a forthcoming paper by Birnstiel, Ricci, Trotta et al. (2010, in preparation)

References

- Andrews, Sean M.; Wilner, D.J.; Hughes, A.M.; Qi, Chunhua; Dullemond, C.P. 2009, ApJ, 700, 1502
 Birnstiel, T., Dullemond, C.P. & Brauer, F. 2010
 Chiang, E.I., & Goldreich, P. 1997, ApJ, 490,368
 Dullemond, C. P., Dominik, C. & Natta, A. 2001, ApJ 560, 957
 Hughes, A.M., Wilner, D.J. & Hogerheijde, M.R. 2008, ApJ, 678,1119
 Isella, A., Carpenter J.M., Sargent A.I., 2009, ApJ, 701, 260
 Isella, A., Carpenter, J.M., Sargent, A.I., 2010
 Lynden-Bell, D. & Pringle, J.E. 1974, MNRAS, 168, 603
 Pollack, J.B., Hollenbach, D., Beckwith, S., Simonelli, D.P., Roush, T. & Fog, W. 1994, ApJ 421,615
 Ricci, L., Testi, L., Natta, A., Neri, R., Cabrit, S. & Herczeg, G.J. 2010